ARTICLE
Journal of Cellular Biochemistry 112:1295–1310 (2011)

Journal of Cellular Biochemistry

Two Nucleus-Localized CDK-Like Kinases With Crucial Roles for Malaria Parasite Erythrocytic Replication Are Involved in Phosphorylation of Splicing Factor

Shruti Agarwal,[1,2] Selina Kern,[1] Jean Halbert,[2,3] Jude M. Przyborski,[4] Stefan Baumeister,[4] Thomas Dandekar,[5] Christian Doerig,[2,3] and Gabriele Pradel[1*]

[1] *Research Center for Infectious Diseases, University of Würzburg, Josef-Schneider-Strasse 2, Building D15, 97080 Würzburg, Germany*

[2] *INSERM U609, Wellcome Centre for Molecular Parasitology, Glasgow Biomedical Research Centre, 120 University Place, University of Glasgow, Glasgow G12 8TA, UK*

[3] *INSERM U609, Global Health Institute, Ecole Polytechnique Fédérale de Lausanne (EPFL), Station 19, 1015 Lausanne, Switzerland*

[4] *Department of Parasitology, Philipps University Marburg, Karl-von-Frisch-Strasse 8, 35043 Marburg, Germany*

[5] *Bioinformatics, University of Würzburg, Biocenter, 97074 Würzburg, Germany*

ABSTRACT

The kinome of the human malaria parasite *Plasmodium falciparum* comprises representatives of most eukaryotic protein kinase groups, including kinases which regulate proliferation and differentiation processes. Despite extensive research on most plasmodial enzymes, little information is available regarding the four identified members of the cyclin-dependent kinase-like kinase (CLK) family. In other eukaryotes, CLKs regulate mRNA splicing through phosphorylation of Serine/Arginine-rich proteins. Here, we investigate two of the PfCLKs, the Lammer kinase homolog PfCLK-1, and PfCLK-2. Both PfCLKs show homology with the yeast Serine/Arginine protein kinase Sky1p and are transcribed throughout the asexual blood stages and in gametocytes. PfCLK-1/Lammer possesses two nuclear localization signal sites and PfCLK-2 possesses one of these signal sites upstream of the C-terminal catalytic domains. Indirect immunofluorescence, Western blot, and electron microscopy data confirm that the kinases are primarily localized in the parasite nucleus, and PfCLK-2 is further present in the cytoplasm. The two kinases are important for completion of the asexual replication cycle of *P. falciparum*, as demonstrated by reverse genetics approaches. In vitro kinase assays show substrate phosphorylation by the PfCLKs, including the Sky1p substrate, splicing factor Npl3p, and the plasmodial alternative splicing factor PfASF-1. Mass spectrometric analysis of co-immunoprecipitated proteins indicates assembly of the two PfCLKs with proteins with predicted nuclease, phosphatase, or helicase functions. Our data indicate a crucial role of PfCLKs for malaria blood stage parasites, presumably by participating in gene regulation through the post-transcriptional modification of mRNA. J. Cell. Biochem. 112: 1295–1310, 2011.

KEY WORDS: MALARIA; KINOME; mRNA SPLICING; TRANSCRIPTION; SR PROTEIN; GENE REGULATION; PHOSPHORYLATION

With an estimated 250 million cases and a death toll of one million people annually, malaria is one of the most devastating tropical diseases worldwide. In most endemic countries, disease treatment and control measures are undermined by the spread of drug resistance, extreme poverty, and HIV infections. Drug-resistant malaria is primarily caused by *Plasmodium falciparum*, which is prevalent in tropical Africa, the Amazon region and South-East Asia [Hyde, 2005]. The dramatic conditions affecting malaria control measures stress the importance for the design of new antiplasmodial agents.

Additional Supporting Information may be found in the online version of this article.

Grant sponsor: EU 7th Framework Programme; Grant codes: MALSIG, ANTIMAL, EVIMALAR; Grant sponsor: Deutsche Forschungsgemeinschaft; Grant numbers: PR905/1, SFB544/B2, SFB630/C6, SFB593/B7/Z2; Grant sponsor: Inserm, EPFL.

*Correspondence to: Dr. Gabriele Pradel, Research Center for Infectious Diseases, University of Würzburg, Josef-Schneider-Strasse 2/D15, 97080 Würzburg, Germany. E-mail: gabriele.pradel@mail.uni-wuerzburg.de

Received 14 April 2010; Accepted 13 January 2011 • DOI 10.1002/jcb.23034 • © 2011 Wiley-Liss, Inc.
Published online 10 February 2011 in Wiley Online Library (wileyonlinelibrary.com).

The complex life cycle of the malaria parasite, which alternates between the human host and an anopheline mosquito vector, provides multiple target structures for drug design. Particularly plasmodial protein kinases (PKs) have gained increasing attention as potential targets, since the parasite relies on them to regulate growth and differentiation throughout its life cycle. Eukaryotic PKs (ePKs) are important chemotherapy targets in a variety of diseases [Cohen, 2001], and the divergence between plasmodial and human kinases make them highly attractive for the design of novel antimalarial drugs [Doerig, 2004; Doerig et al., 2005; Doerig and Meijer, 2007].

Gene information gained by the sequencing of the *P. falciparum* genome led to the identification of 65 sequences related to ePKs and 21 members of a novel kinase-related family called "FIKKs" after a conserved Phe-Ile-Lys-Lys motif [Ward et al., 2004; Anamika et al., 2005]. Most *P. falciparum* ePKs cluster within the previously defined ePK groups [Hanks and Quinn, 1991]. The ePK group that comprises the largest number of *P. falciparum* kinases is the CMGC [cyclin-dependent (CDK), mitogen-activated (MAPK), glycogen-synthase (GSK3), and cyclin-dependent kinase-like kinases (CLK)] group, members of which are largely implicated in cell proliferation and development.

Whereas plasmodial enzymes of the CDK, MAPK, and GSK3 families have been investigated extensively, very little information is available regarding the fourth family in the CMGC group, the CLKs. In other eukaryotes, CLKs are major regulators of mRNA splicing by phosphorylation of Serine/Arginine-rich (SR) proteins, which function in the RNA processing pathway [reviewed in Huang and Steitz, 2005; Sanford et al., 2005; Godin and Varani, 2007]. Thus, CLKs participate in the control of gene expression, and may be particularly important in malaria parasites, in view of the importance of post-transcriptional regulation of gene expression in these protozoa [Deitsch et al., 2007]. Four kinases cluster within the CLK family, which we call PfCLK-1 (PF14_0431), PfCLK-2 (PF14_0408), PfCLK-3 (PF11_0156), and PfCLK-4 (PFC0105w). PfCLK-1 represents the plasmodial homolog of the mammalian Lammer kinase [Li et al., 2001], which binds to and phosphorylates SR-rich mRNA splicing factors [Colwill et al., 1996; Nayler et al., 1997]. PfCLK-4 was recently described as splicing-related PK PfSRPK1, which phosphorylates the parasite splicing factor SR1 [Dixit et al., 2010]. We here focus on the kinases PfCLK-1/Lammer and PfCLK-2 and provide a detailed characterization of the two kinases in the blood stages of the malaria parasite *P. falciparum*.

MATERIALS AND METHODS

GENE IDS

The following PlasmoDB gene identifiers are assigned to the proteins investigated in this study: Pf39, PF11_0098; PfAMA-1, PF11_0344; PfASF-1, PF11_0205; PfCCp1, PF14_0723; PfCLK-1/Lammer, PF14_0431; PfCLK-2, PF14_0408; Pfs25, PF10_0303.

BIOINFORMATICS

The following computer programmes and databases were used for the in silico studies: For gene sequence annotation, PlasmoDB (www.plasmodb.org) [Fraunholz and Roos, 2003] and NCBI sequence analysis software and databanks [Sayers et al., 2010] were used, and for prediction of phophorylation sites, the software kinasephos (www.kinasephos.mbc.nctu.edu.tw) was used. Prediction of nuclear localization signal sites involved the PredictNLS server (www.cubic.bioc.columbia.edu/predictNLS) and the program LOCtree [Nair and Rost, 2005]. Multiple sequence alignment involved ClustalW (www.ebi.ac.uk/clustalw) and formatting of multiple sequence alignments according to standard methods (www.espript.ibcp.fr) [Higgins et al., 1996]. Deduction of catalytic domains used sequence and domain analysis including the SMART databank (www.smart.embl-heidelberg.de) [Letunic et al., 2006]. Alignment of catalytic domains was obtained using the ClustalW multiple sequence alignment program.

PARASITE CULTURE

Asexual parasites and mature gametocytes of the *P. falciparum* NF54 isolate, of the 3D7 strain or of the gametocyte-less F12 strain were cultivated in vitro as described [Ifediba and Vanderberg, 1981]. Gametogenesis was induced by incubating mature gametocyte cultures in 100 μM xanthurenic acid for 15 min at room temperature (RT). Zygote formation was achieved by incubation of emerged gametes in human serum overnight at RT. Zygotes and gametocytes were enriched via centrifugation over 6/11/16% Accudenz gradients and parasites were collected at the gradient interfaces [Pradel et al., 2004]. For synchronization, parasite cultures with 3–4% ring stages were centrifuged to obtain the pellet, which was resuspended in five times volume of 5% prewarmed sorbitol w/v (AppliChem) in RPMI medium (Invitrogen) and incubated at RT for 10 min. The cells were washed once with RPMI medium to remove the sorbitol, diluted to 5% hematocrit and cultured as described above.

PARASITE EXTRACT PREPARATION

Parasite cultures with 6–8% parasitemia were lysed in 0.15% saponin/PBS. The pellet was resuspended in 200 μl lysis buffer [Nunes et al., 2007] and sonicated with 50% amplitude and 50 cycles. Centrifugation was performed at 13,000*g* and 4°C for 10 min. The supernatant was collected and total protein concentration was measured by Bradford assay (Bio-Rad). For the preparation of nuclear extract, parasite pellet was washed with PBS, resuspended in Buffer A (10 mM HEPES, pH 7.9, 10 mM KCl, 0.1 mM EDTA, 1 mM DTT, 10% IGEPAL, and 1× complete protease inhibitor cocktail; Roche Diagnostics) and incubated at RT for 10 min followed by centrifugation at 13,000*g* for 10 min at 4°C. The resultant pellet was resuspended in Buffer B (20 mM HEPES, pH 7.9, 0.4 M NaCl, 1 mM EDTA, 10% glycerol, 1 mM DTT, and 1× complete protease inhibitor cocktail). The resuspended pellet was vigorously shaken for 2 h at 4°C and centrifuged at 13,000*g* and 4°C for 5 min. The supernatant representing the nuclear fraction was then used for further analyses. The purity of the nuclear fraction was confirmed by Hoechst labeling of nuclei. Further, Western blot analysis confirmed that the nuclear fraction was devoid of the parasite digestive enzyme plasmepsin 2 [Francis et al., 1994], which was used as a marker for the cytosolic fraction (data not shown).

RNA ISOLATION AND TRANSCRIPT LEVEL ANALYSIS

RNA from synchronized wild-type (WT) *P. falciparum* 3D7 strain was isolated using the TRIzol reagent (Invitrogen, Karlsruhe) according to the manufacturer's protocol. Contamination from gDNA was removed by treatment with RNase-free DNase I (Invitrogen) followed by phenol/chloroform extraction and ethanol precipitation. cDNA was synthesized using a Supercript II cDNA synthesis kit (Invitrogen). Real-time RT-PCR was performed for quantitation of the transcript expression using SYBR-Green mix (Bio-Rad) [Pradel et al., 2004] and samples were subjected to a real-time thermocycler (iCycler iQ^{TM} Real-Time PCR; Bio-Rad), using the following sequence-specific primers: PfCLK-1/Lammer forward primer 5′-GAT ACG CAT TTT GGA CAA-3′ and reverse primer 5′-TTC CCA TCT TGA GAT GGA-3′; PfCLK-2 forward primer 5′-AGA TGC TTG GAA ACA ACC-3′ and reverse primer 5′-GCC AAA GTT AGG TGA TGA-3′. Pf39 forward primer 5′-CTT GAA CAC CAT GAT GTA-3′ and reverse primer 5′-TCC ACT TTC ATG AGC AGG-3′; PfAMA-1 forward primer 5′-GGA TTA TGG GTC GAT GGA-3′ and reverse primer 5′-GAT CAT ACT AGC GTT CTT-3′; PfCCP1 forward primer 5′-GAA GAT GGA GAT GGG AAA-3′ and reverse primer 5′-GCT GTT CAA ATT CCC ATC-3′; Pfs25 forward primer 5′-CCA TGT GGA GAT TTT TCC-3′ and reverse primer 5′-TAC ATT GGG AAC TTT GCC-3′. Primers were used at a concentration of 1 pm/μl and primer-only reaction without cDNA served as the negative control.

RECOMBINANT PROTEIN EXPRESSION

The design of recombinant protein construct for PfCLK-1/Lammer was guided by domain architecture determinations, and recombinant protein was produced corresponding to the catalytic domain (Fig. 1A). Recombinant protein was expressed as fusion protein with a GST-tag using the pGEX 4T1 vector (Amersham Bioscience). Cloning was mediated by the addition of *Sal*I/*Not*I restriction sites to the ends of PCR-amplified gene fragments, using forward primer 5′-TAGGTCGACTCGTCCATTTTAGTTGGAAG-3′ and reverse primer 5′-TAGCGGCCGCTTACGGTCGAAGTGTTGGATC-3′ (restriction sites underlined). Recombinant protein was expressed in BL21 (DE3) RIL cells according to the manufacturer's protocol (Stratagene), resulting in a 62 kDa GST-fusion protein (Supplemental Fig. 1A), which was purified from bacterial extracts using glutathione-sepharose according to the manufacturer's protocol (GE Healthcare). Similarly, cloning of gene fragments for the alternative splicing factor PfASF-1 was conducted using forward primer 5′-AAGAATTC-ATGAAAAAGTTAATTAATTGTGGC-3′ and reverse primer 5′-TT-GCGGCCGCTTAATTTAGTTCCTTTGGAGA-3′ via *Eco*RI/*Not*I restriction sites. Bacterial expression resulted in a GST-fusion protein of 48 kDa (Supplemental Fig. 1B). GST-tag alone was expressed as previously described [Simon et al., 2009].

MOUSE ANTISERA

GST-tagged recombinant PfCLK-1/Lammer protein was purified by glutathione beads according to the manufacturer's protocol (Sigma–Aldrich). Specific immune sera against the PfCLK-1/Lammer catalytic domain were generated by the immunization of 6-week-old female NMRI mice (Charles River Laboratories) with 100 μg recombinant protein emulsified in Freund's incomplete adjuvant (Sigma–Aldrich) followed by a boost after 4 weeks. Mice were anesthesized by intraperitoneal injection of a mixture of ketamine and xylazine according to the manufacturer's protocol (Sigma–Aldrich), and immune sera were collected 10 days after the second immunization via heart puncture. The antisera recognized the cognate recombinant protein (Supplemental Fig. 1A) as well as the endogenous protein in asexual and gametocyte extracts as investigated by Western blot analysis and immunofluorescence assay (Figs. 1C and 2). Sera from non-immunized mice served as control for all antibody reagent studies. For PfCLK-2, antisera from two mice were generated against the peptide sequence CISYNE-KENKYNDQD upstream of the catalytic domain (Biogenes). Housing and handling of the animals followed the guidelines of the animal welfare committee of the government of Lower Franconia.

REVERSE GENETICS PLASMID CONSTRUCTION

Reverse genetics approaches were performed as described [Dorin-Semblat et al., 2007, 2008]. The two constructs for gene disruptions, pCAM-BSD-CLK1-KO and pCAM-BSD-CLK2-KO, were designed such that homologous integration would lead to disruption of the kinase domains (Supplemental Fig. 2). Primers introduced *Bam*HI/*Not*I restriction site in the PCR fragments, which included a stop codon and were ligated to the *Bam*HI/*Not*I-cut pCAM-BSD vector. Vector pCAM-BSD-CLK1-KO contained a 543 bp fragment, which was PCR-amplified from *P. falciparum* NF54 isolate gDNA template using gene-specific forward primer 5′-GGATCCTTTGGTAGAGTTT-TATTATGTCAA-3′ and reverse primer 5′-GCGGCCGCTTAAGCTC-GATATTGTCTAGT-3′. Vector pCAM-BSD-CLK2-KO contained a 512 bp fragment amplified from NF54 isolate gDNA template using forward primer 5′-GGATCCTTGTTAGAACTCATGGTC-3′ and reverse primer 5′-GCGGCCGCTTACACATTCGATGTCTTTTC-3′. C′-terminal Myc-tagged kinases were generated by inserting 600–800 bp of the homologous 3′-end of the coding gene sequence lacking a stop codon into the pCAM-BSD vector containing double Myc-tag and 3′UTR from *P. berghei* DHFR-ts (Supplemental Fig. 2). Vector pCAM-BSD-CLK1-Myc contained a fragment of 873 bp amplified from 3D7 isolate gDNA template using forward primer 5′-CTGCAGCGCTCAGCTAAAATTGAA-3′ and reverse primer 5′-AGATCTATAGTACTCATAATTTTCTTCAAGGAACTTGTGC-3′. The vector pCAM-BSD-CLK2-Myc contained a fragment of 621 bp amplified from 3D7 isolate gDNA using forward primer 5′-CTGCAGCAAACTCGATCTTATAGA-3′ and reverse primer 5′-GGATCCTAAACCGTCTTTATACAA-3′. *Pst*I/*Bam*HI-digested PCR products were ligated into *Pst*I/*Bam*HI-cut pCAM-BSD Myc-tagged vector.

PARASITE TRANSFECTION AND GENOTYPE CHARACTERIZATION

Ring stage parasites of *P. falciparum* strain 3D7 were electroporated with 60 μg of the respective plasmid DNA as described [Sidhu et al., 2005]. Blasticidin (Invitrogen) was added to a final concentration of 2.5 μg/ml, starting at 48 h after transfection. Resistant parasites appeared 3–4 weeks later. After 60–90 days of drug pressure, the respective cultures were investigated for plasmid-integration by a diagnostic PCR assay. The following listed primers corresponding to the *PfCLK1/Lammer* or *PfCLK-2* loci and from the flanking regions of pCAM-BSD vector were used for the investigation of WT loci, 5′ and 3′ integrations and for the presence of episome (primer locations

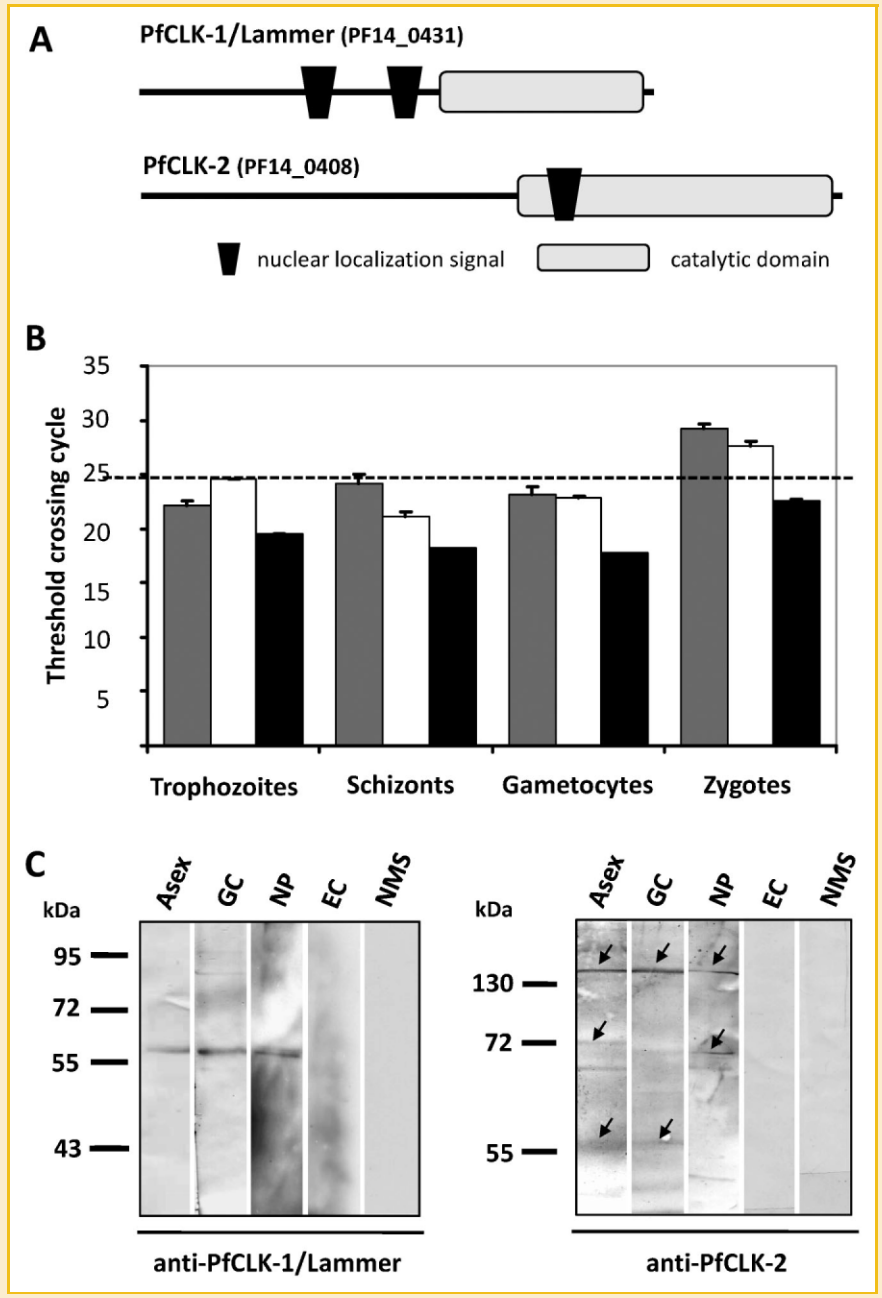

Fig. 1. Schematic of PfCLKs and blood stage-specific expression. A: The Serine/Threonine kinases PfCLK-1/Lammer (PF14_0431; 107 kDa) and PfCLK-2 (PF14_0408; 150 kDa) posses two putative nuclear localization signal sites and one nuclear localization signal site, respectively, upstream to the C-terminal catalytic domains. B: Real-time RT-PCR analysis showed transcript expression of *PfCLK-1/Lammer* (gray bar) and *PfCLK-2* (white bar) in the asexual blood stages as well as in gametocytes. Threshold crossing cycle refers to the approximate midpoint cycle of the linear portion of product amplification, a threshold crossing cycle number above 25 (dotted line) indicates low transcript abundance. The following stage-specific positive controls were used (black bar): *Pf39* (trophozoites); *AMA-1* (schizonts); *PfCCp1* (gametocytes); *Pfs25* (zygotes). C: Western blot analyses on parasite lysates, using mouse antisera against PfCLK-1/Lammer and PfCLK-2, revealed protein expression in the parasite blood stages. Labeling for PfCLK-1/Lammer visualized a protein band with an approximate molecular weight of 60 kDa in asexual blood stage parasites (ASEX; gametocyte-less strain F12) and in gametocytes (GC; gametocyte-producing strain NF54). Blotting with anti-PfCLK-2 antibody revealed a full size protein band at 150 kDa, as well as lower molecular weight protein bands at 70 and 55 kDa (arrows). The kinases were further detected in a nuclear pellet fraction (NP). Lysates of uninfected erythrocytes (EC) and blotting of F12 lysate with non-immunized mouse sera (NMS) were used for negative control.

are shown in Supplemental Fig. 2): pCAM-BSD-CLK1-KO gene-specific primers: forward primer WT1 5′-TCGTCCATTTTAGTTG-GAAG-3′ and reverse primer WT2 5′-CGGTCGAAGTGTTGGATC-3′; pCAM-BSD-CLK1-KO vector primers: forward primer EP1 5′-TATTCCTAATCATGTAAATCTTAAA-3′ and reverse primer EP2 5′-CAATTAACCCTCACTAAAG-3′. pCAM-BSD-CLK1-Myc gene-specific primer: forward primer WT1 5′-AGAGTTTTATTATGTCAA-3′ and reverse primer WT2 5′-GATGTATCTAGTGAT-3′; pCAM-BSD-

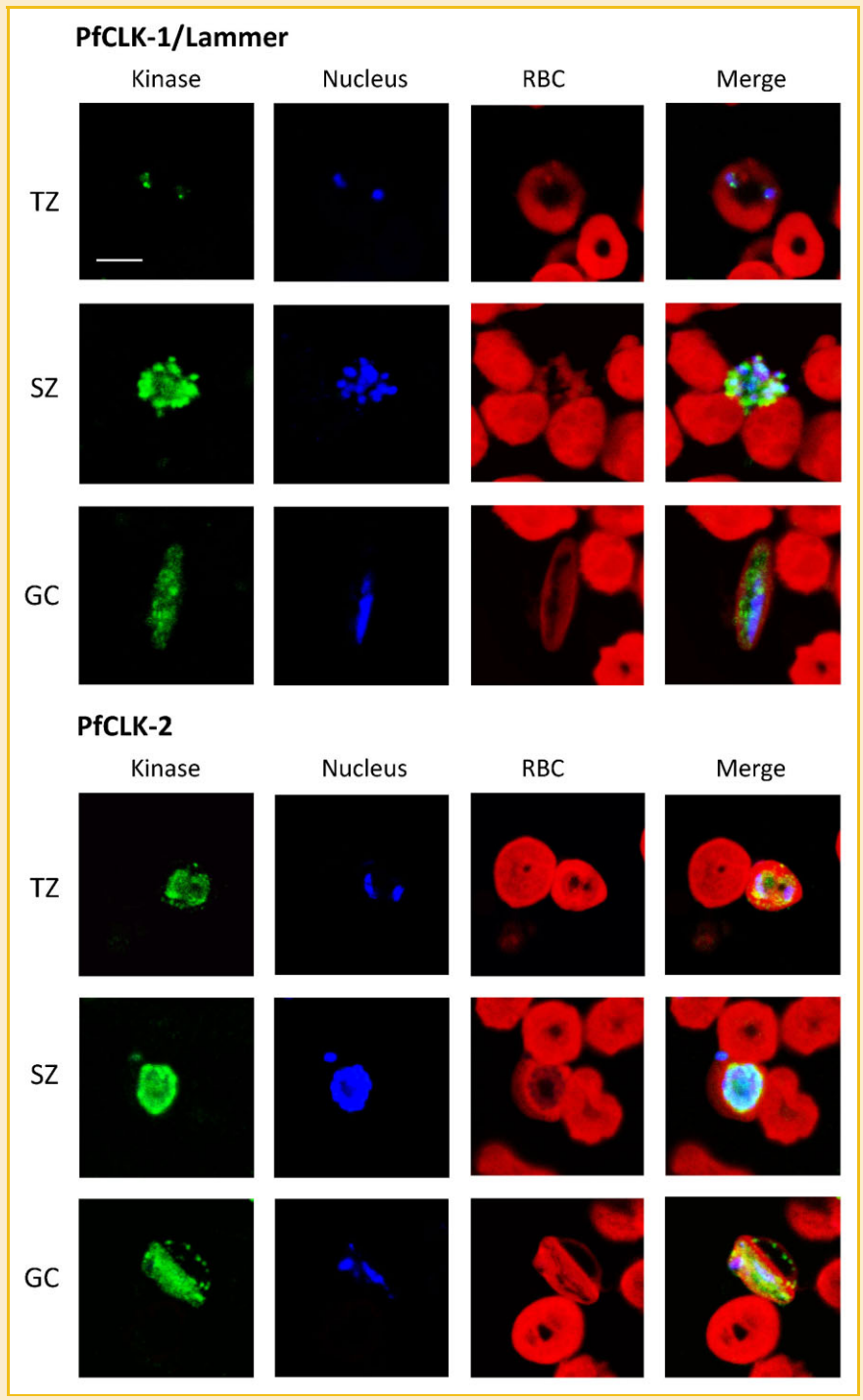

Fig. 2. Blood stage-specific PfCLK expression and co-localization with the parasite nucleus. Indirect immunofluorescence assay using anti-PfCLK-1/Lammer antibody showed distinct punctate protein expression in association with the nucleus of trophozoites (TZ) and schizonts (SZ). In gametocytes (GC) PfCLK-1/Lammer expression was not restricted to the nucleus, but also present in the cytoplasm. PfCLK-2 was present in nucleus and cytoplasm of asexual parasites and gametocytes. In gametocytes, an additional labeling of the erythrocyte hem in a punctate pattern was observed. Kinase labeling was visualized with AlexaFluor488 secondary antibody (green), nuclei were highlighted by Hoechst staining (blue), red blood cells (RBC) were counterstained with Evans Blue (red). Bar: 5 μm.

CLK1-Myc vector primers: forward primer EP1 5′-TATTCCTAA-TCATGTAAATCTTAAA-3′ and reverse primer EP2 5′-CAATTAA-CCCTCACTAAAG-3′. pCAM-BSD-CLK2-KO gene-specific primers: forward primer WT1 5′-TCACACAAGTATTCCTACCA-3′ and reverse primer WT2 5′-TTATGGCTGAAGCCATGGGTG-3′; pCAM-BSD-CLK2-KO vector primers: forward primer EP1 5′-TATTCCTAA-TCATGTAAATCTTAAA-3′ and reverse primer EP2 5′-CAAT-TAACCCTCACTAAAG-3′. pCAM-BSD-CLK2-Myc gene-specific

primers: forward primer WT1 5′-TTGTTAGAACTCATGGTC-3′ and reverse primer WT2 5′-GAGAAATGTTATTTCCACT-3′; pCAM-BSD-CLK2-Myc vector primers: forward primer EP1 5′-TATTCCTAAT-CATGTAAATCTTAAA-3′ and reverse primer EP2 5′-CAATTAA-CCCTCACTAAAG-3′.

SOUTHERN BLOT ANALYSIS

gDNA was isolated from asexual 3D7 WT parasites and PfCLK-Myc mutants after saponin lysis using a DNA purification kit (Epicentre Biotechnologies) as per manufacturer's instructions. Restriction digest assays diagnostic of WT versus Myc-tagged loci were guided by analysis of the genome nucleotide sequence of the extended gene loci (for location of restriction sites, see Figs. 5A and 6A). An amount of 2.5 μg of gDNA was digested with *Eco*RI for analysing *PfCLK-1/Lammer* and with *Eco*RV and *Bgl*II for *PfCLK-2* locus. Restriction digested products were separated by 0.7% agarose gel electrophoresis and transferred to Hybond N+ membrane (Amersham Bioscience). A hybridization probe of approximately 500 bp was used for detection of integration in *PfCLK* genes. The probe for *PfCLK-1/Lammer* was amplified by PCR from 5′ to the integration using the following primers: forward primer 5′-TACTACGATACGC-GAAAT-3′ and reverse primer 5′-GCTTCGGGATCTACTTCT-3′. For *PfCLK-2*, the insert from the pCAM-BSD vector was used as the probe (see "a" in Figs. 5A and 6A). The spin-purified hybridization probe was labeled with digoxygenin (DIG) and Southern blot hybridization was performed according to the manufacturer's instructions using the DIG High Prime DNA Labelling and Detection Starter Kit II (Roche Diagnostics).

WESTERN BLOT ANALYSIS

Western blot analyses were performed on lysates of *P. falciparum* gametocyte-producing isolate NF54 and strain 3D7, gametocyte-less strain F12, as well as on the two PfCLK-Myc mutant lines. For generation of lysates, parasite pellets after saponin lysis or Accudenz gradient-enriched gametocytes were resuspended in PBS and SDS–PAGE loading buffer. Parasite proteins were separated by SDS–PAGE electrophoresis and transferred to Hybond ECL nitrocellulose membrane (Amersham Biosciences) according to the manufacturer's instructions. Membranes were blocked for non-specific binding by incubation in Tris-buffered saline containing 5% skim milk and 1% BSA fraction V, followed by immune recognition for 2 h at RT with mouse immune sera specific to the PfCLKs or rabbit antibody directed against the Myc-tag (Myc-Tag 71D10, Cell Signaling Technology). After washing, membranes were either incubated for 1 h at RT with an alkaline phosphatase-conjugated secondary antibody (Sigma–Aldrich) and developed in a solution of nitroblue tetrazolium chloride (NBT) and 5-brom-4-chlor-3-indoxylphosphate (BCIP; Sigma–Aldrich) for 5–30 min, or with horseradish peroxidase-conjugated secondary antibody (Dako) following incubation of the blot with Detection reagent (250 mM luminol, 90 mM *p*-coumaric acid, 1 M Tris–HCl, pH 8.5, and 30% H_2O_2) for 1 min. Chemiluminescence was measured via autoradiography with an average exposure time of 10 min. Scanned blots were processed using Adobe Photoshop CS software.

INDIRECT IMMUNOFLUORESCENCE ASSAY

Parasite preparations for immunofluorescence microscopy included mixed asexual stages or mature gametocytes of the *P. falciparum* NF54 isolate as well as PfCLK-Myc blood stages. Preparations were air dried on slides and fixed for 10 min in −80°C methanol. For membrane permeabilization and blocking of non-specific binding, fixed cells were incubated in 0.01% saponin, 0.5% BSA, and 1% neutral goat serum (Sigma–Aldrich) in PBS for 30 min. Preparations were then incubated for 2 h at 37°C with kinase-specific mouse immune sera or rabbit anti-Myc antibody. Binding of primary antibody was visualized using fluorescence-conjugated goat anti-mouse or anti-rabbit antibodies (Alexa Fluor 488; Molecular Probes, Karlsruhe). Counterstaining of erythrocytes was performed using 0.05% Evans Blue in PBS (Sigma–Aldrich). Nuclei were highlighted by incubating the specimens with Hoechst nuclear stain (Molecular Probes) for 1 min. Labeled specimens were examined by confocal laser scanning microscopy using a LEICA TCS SP5 (Fig. 2) or a Zeiss Axiolab fluorescence microscope in combination with a Zeiss AxioCam ICc1 camera (Supplemental Fig. 4). Digital images were processed using Adobe Photoshop CS software.

IMMUNOELECTRON MICROSCOPY

Asexual parasites of *P. falciparum* NF54 or of the PfCLK-Myc mutants were fixed in 4% paraformaldehyde in PBS for 1 day and treated with 50 mM NH_4Cl in PBS for 15 min to block aldehyde groups. Specimens were dehydrated in increasing concentrations of ethanol at −25°C and then incubated for 1 h in a 1:1 mixture of 100% ethanol and LR White (Scientific Services) at 4°C. Specimens were subsequently embedded in LR White at 40°C for 3 days. Ultrathin sections of the respective specimens were then subjected to post-embedding labeling. Samples were blocked in 1% BSA and 0.1% Tween 20 in PBS for 10 min prior to immunolabeling with mouse anti-PfCLK antisera or rabbit anti-Myc antibodies. Binding of primary antibody was visualized using 12 nm gold-conjugated goat anti-mouse or anti-rabbit secondary antibodies (Dianova). Ultrathin sections were subsequently post-fixed with 1% glutaraldehyde in PBS and post-stained with 2% uranylacetate. Photographs were taken with a Zeiss EM10 transmission electron microscope and scanned images were processed using Adobe Photoshop. For quantification of gold labeling, 10 representative sections of blood stage trophozoites or early schizonts were chosen for each setting. Gold particles were counted for the total area of the parasite section and for selected organelles separately. For background labeling control, gold particles of a proportional area of an adjacent uninfected erythrocyte section were counted.

CO-IMMUNOPRECIPITATION

Parasite pellets obtained from WT or Myc-tagged PfCLKs after saponin lysis were resuspended in 200 μl lysis buffer and sonicated with 50% amplitude and 50 cycles followed by centrifugation at 13,000*g* and 4°C for 10 min. Prepurification of lysate was done by consecutive incubation with 5% (v/v) non-immunized mouse sera and 20 μl of protein G-beads (Santa Cruz Biotechnology) for 30 min each at 4°C. After centrifugation, the supernatant was incubated for 1 h at 4°C with 16 μl of mouse anti-PfCLK antisera or with 2 μl

anti-Myc-tag antibody. A volume of 20 μl protein G-beads was added and incubated for another hour. The beads were centrifuged, washed with PBS, and either mixed with an equal volume of loading buffer and loaded onto a 12% SDS gel for Western blotting or employed in kinase activity assay (see below). Gels were subsequently stained with colloidal Coomassie. Selected protein bands were then subjected to mass spectrometry (see below).

KINASE ACTIVITY ASSAY

Kinase reaction of 30 μl was carried out in a standard kinase buffer [20 mM Tris–HCl, pH 7.5, 20 mM $MgCl_2$, 2 mM $MnCl_2$, 10 mM NaF, 10 mM β-glycerophosphate, 10 μM ATP, and 0.1 MBq (γ-32P) ATP], using co-immunoprecipitated endogenous proteins as well as 5 μg of substrate. In the assays, exogenous substrates (histone H1, myelin basic protein (MBP), and casein; Sigma–Aldrich), recombinant GST-tagged Npl3p (kindly provided by G. Ghosh, University of California) and recombinant GST-tagged PfASF-1, both purified by glutathione beads according to the manufacturer's protocol (Sigma–Aldrich) were used. Reactions were incubated at 37°C for 1 h under constant agitation and terminated by addition of reducing Laemmli buffer for 5 min at 100°C. Samples were separated on 12% SDS–PAGE, dried, and exposed to X-ray films for 48–60 h at −20°C.

MASS SPECTROMETRY

The protein bands were subjected to in-gel trypsin digestion before mass spectrometry analysis as described previously [Hellmann et al., 1995]. The peptide mixtures from the tryptic digests were desalted and concentrated using ZipTips™ columns made from the reverse chromatography resins Poros and Oligo R3 (Applied Biosystems). The bound peptides were washed with a solution of 0.5% formic acid and eluted from the column in 1 μl of 33% (v/v) acetonitrile/0.1% trifluoroacetic acid solution saturated with α-cyano-4-hydroxy-cinnamic acid (Bruker Daltonics) directly onto a MALDI target plate and air dried before analysis in the mass spectrometer. Measurement was performed on an Ultraflex-TOF TOF tandem mass spectrometer (Bruker Daltonics). Peptide mass fingerprint spectra were acquired in the reflectron positive mode with a pulsed extraction using approximately 100 laser shots. The spectra were acquired after an external calibration using reference peptides (Peptide mixture II, Bruker Daltonics). After internal calibration using trypsin autolysis peaks as internal standards (842.5100 and 2211.1046 Da), the monoisotopic masses were assigned and processed using Biotools™ and FlexAnalysis™ software (Bruker Daltonics). Subsequently they were submitted to the Mascot program (www.matrixscience.com) for searches against the non-redundant NCBI database. The parameters used in the Mascot peptide mass fingerprint searches were as follows: Taxonomy, *P. falciparum* and *Homo sapiens*; search all molecular masses and all isoelectric points; allow up to one missed proteolytic cleavage site and a peptide mass tolerance of 100 ppm. Methionine oxidation was considered as an optional modification and cysteine carbamidomethylation as a fixed modification in all the searches. Matches to human proteins were considered unambiguous when the probability score was significant using the Mascot score with a P-value <0.05.

RESULTS

PfCLK-1/LAMMER AND PfCLK-2 EXHIBIT HOMOLOGY TO YEAST SKY1P

PfCLK-1/Lammer and PfCLK-2 are annotated in PlasmoDB (www.plasmodb.org) as "putative Serine/Threonine kinases, with a possible additional function of Tyrosine phosphorylation". PfCLK-1/Lammer and PfCLK-2 are large polypeptides, with predicted sizes of 881 amino acids (107 kDa) and 1,268 amino acids (150 kDa), respectively. In both proteins, the ~300 residue predicted kinase catalytic domain is located at the C-terminus. In silico analysis of gene sequences revealed two nuclear localization signal sites for PfCLK-1/Lammer and one signal for PfCLK-2, located upstream of the C-terminal catalytic domains, and predicted a localization of the kinases within nuclear speckles (Fig. 1A).

The catalytic domain sequences of PfCLK-1/Lammer and PfCLK-2 were aligned with the kinase Sky1p of *Saccharomyces cerevisae* [Nolen et al., 2001], based on (i) previous phylogenetic analysis demonstrating relatedness of PfCLK1 and PfCLK2 with SR kinases from other eukaryotes [Ward et al., 2004], and (ii) the high score obtained upon BLASTP analysis of the yeast proteome with PfCLK-2 (not shown). Sky1p is a well studied non-essential SR protein-phosphorylating kinase with known structure (pdb code 1HOW) [Nolen et al., 2001] that has been reported to be involved in mRNA splicing and mRNA transport in yeast [Siebel et al., 1999]. Sequence alignment confirmed the presence of all conserved kinase domains in both PfCLKs (Supplemental Fig. 3). This includes the presence of the conserved sequence DLKPEN starting with the catalytic Aspartate 126. The activation loop lies between positions 169 and 193, starting with Aspartate 169 and ending with the motifs APE in PfCLK-1/Lammer and SPE in PfCLK-2 and Sky1p. The glycine triad GXGXXG implicated in ATP-binding is present at positions 8–13 for PfCLK-1/Lammer and is substituted in Sky1p with GXGXXS, but not present in PfCLK-2.

Sequence alignment further revealed matches between substrate-binding residues of the kinases with the substrate-binding site of Sky1p. These residues include Arginine 187, Tyrosine 189, Arginine 190, and Glutamate 215 (Supplemental Fig. 3). Notably, the yeast Sky1p kinase has a specific and well-studied substrate, the nucleocytoplasmic shuttle protein Npl3p [Siebel et al., 1999; Lukasiewicz et al., 2007].

PfCLK-1/LAMMER AND PfCLK-2 LOCALIZE TO THE NUCLEUS OF PARASITE BLOOD STAGES

Transcript expression for the two kinases was investigated by real-time RT-PCR in four parasite stages, that is, trophozoites, schizonts, gametocytes, and zygotes (Fig. 1B). Threshold crossing cycle numbers for each of the stages were compared to the expression of respective stage-specific genes, that is, *Pf39* for trophozoites [Templeton et al., 1997], *AMA-1* for schizonts [Peterson et al., 1989], *PfCCp1* for gametocytes [Pradel et al., 2004], and *Pfs25* for zygotes [Kaslow et al., 1988]. Real-time RT-PCR data confirmed PlasmoDB microarray data showing that *PfCLK-1* and *PfCLK-2* mRNA is present in the asexual blood stages and gametocytes, with lower transcript levels in the zygote stage (Fig. 1B).

We subsequently studied expression of the two kinases at the protein level. We raised polyclonal mouse antisera against a recombinantly expressed portion of the PfCLK-1/Lammer catalytic domain and a polyclonal mouse antisera against a peptide sequence upstream of the PfCLK-2 catalytic domain. In accord with the above data on transcript expression, Western blot analyses revealed protein expression for both enzymes in lysates of asexual stages (using the gametocyte-less strain F12) and of gametocytes (using the gametocyte-producing strain NF54; Fig. 1C). Mouse antisera against PfCLK-1/Lammer detected a protein band in both lysates at approximately 60 kDa (Fig. 1C). In some cases, an additional faint protein band at the predicted molecular weight of 107 kDa was detectable (data not shown), suggesting that most of PfCLK-1/Lammer protein is present in a processed 60 kDa form. The 60 kDa protein band was also detected in a nuclear pellet fraction of asexual parasites (Fig. 1C). Further, mouse antisera against PfCLK-2 detected the kinase in asexual parasite as well as in gametocyte lysates and in the nuclear pellet fraction (Fig. 1C). The detected protein bands migrated at the expected molecular weight of 150 kDa. Additional bands with approximate molecular weights of 70 and 55 kDa were detectable, indicating protein processing or degradation (Fig. 1C). No protein bands were detected with either antisera in lysates of uninfected erythrocytes. Further, non-immunized mouse sera did not result in any labeling, when used on the F12 parasite lysates (Fig. 1C).

Protein expression of the two kinases was further investigated by immunofluorescence assay on methanol-fixed blood stage cultures of strain NF54. Immunolabeling with the mouse antisera against PfCLK-1/Lammer revealed a distinct punctate expression within the nuclei of trophozoites and of schizonts (Fig. 2). In gametocytes, on the other hand, PfCLK-1/Lammer labeling was more diffuse and not restricted to the nucleus (Fig. 2). The anti-PfCLK-2 antibody labeled the nuclei as well as the cytoplasm of asexual blood stages, particularly of schizonts (Fig. 2). Similarly, nucleus and cytoplasm were P labeled in gametocytes. Here, in some cases an additional punctate labeling of the erythrocyte hem was observed (Fig. 2). No labeling was detected with non-immunized mouse sera (data not shown).

Subcellular localization of the two kinases was subsequently investigated by immunoelectron microscopy, using gold-conjugated secondary antibody. When ultrasections were probed with antibodies against PfCLK-1/Lammer, gold-labeling was mostly found in the nuclei, which are surrounded by a double membrane and often display an electron-denser matrix than the parasite cytoplasm (Fig. 3A). PfCLK-1/Lammer labeling was to a lower extent also present in the cytoplasm of malaria parasites. In some occasions, intense gold-labeling was observed at the passage between nucleus and cytoplasm (Fig. 3B). Gold-labeling for PfCLK-2 was detected both in the nuclei and the cytoplasm of blood stage parasites (Fig. 3C). Again gold-labeling was in some occasions detectable at the passage between nucleus and cytoplasm (Fig. 3D). No significant labeling was found in the parasite rhoptries and in the food vacuole, nor in the erythrocyte cytoplasm. Further, incubation with secondary antibody alone did not lead to any gold-labeling (data not shown).

Immunoelectron gold-labeling was subsequently quantified in 10 representative sections of trophozoites and schizonts for each setting and compared to potential background labeling in similar areas of adjacent uninfected erythrocytes (Table I). Quantification of gold particles confirmed kinase-specific labeling of blood stage parasites, which was standing out from background labeling in erythrocytes. Labeling of PfCLK-1/Lammer was particularly found in the parasite nuclei, while PfCLK-2 labeling was further present in the parasite cytoplasm, resulting in a significantly higher parasite-specific total number of gold particles for anti-PfCLK-2 antibody-treated ultrasections compared to the number of gold particles for anti-PfCLK-1/Lammer antibody-treated section. In the parasite rhoptries and the food vacuole, gold particles were only found occasionally, confirming that these structures do not label for the kinases (Table I).

PfCLK-1/LAMMER AND PfCLK-2 ARE CRUCIAL FOR ERYTHROCYTIC SCHIZOGONY

To investigate whether the PfCLK kinases are crucial for blood stage replication, we attempted to individually disrupt the *PfCLK-1/Lammer* and *PfCLK-2* genes by single cross-over homologous recombination, using the pCAM-BSD vector [Sidhu et al., 2005]. The knock-out (KO) vector contained an insert corresponding to the central portion of the kinase catalytic domain, as well as a cassette conferring resistance to blasticidin. Integration into the respective PfCLK gene would result in a disrupted (pseudo-diploid) locus, in which the ATP-binding region and the proline-glutamate (PE) motif of the catalytic domain are separated (Supplemental Fig. 2).

The pCAM-BSD-based PfCLK-KO vectors for *PfCLK-1/Lammer* and *PfCLK-2* were electroporated into ring stage parasites of strain 3D7 and populations of blasticidin-resistant parasites were obtained. However, these parasites contained only non-integrated episomes, and no integration of the respective PfCLK-KO vector could be detected for either of the two kinase genes by diagnostic PCR (Fig. 4, left panels), even after prolonged culture (20 weeks). Noteworthy, isochronously the locus of another *P. falciparum* kinase, PFC0485w (termed PKRP in *P. berghei* [Purcell et al., 2010]), was disrupted by the same strategy (S. Agarwal, C. Doerig, R. Schillig, G. Pradel, unpublished observations).

To verify that the genomic loci for *PfCLK-1/Lammer* and *PfCLK-2* were accessible for recombination, we generated pCAM-BSD-based vectors that contained an insert homologous to the 3′-end of the respective kinase gene fused to the sequence encoding a Myc-epitope, followed by the 3′-untranslated region from the *P. berghei dhfr-ts* gene (Supplemental Fig. 2). Single cross-over homologous integration of the vector would result in a complete kinase gene followed by a 3′-located Myc-sequence. This recombination is predicted not to cause loss of function of the gene product, but to generate a functional enzyme carrying a Myc-tag at its C-terminus.

The Myc-tag vectors for *PfCLK-1/Lammer* and *PfCLK-2* were electroporated into ring stage cultures and treated with blasticidin as described above. No growth differences between cultures electroporated with the Myc-tag vectors and cultures electroporated with the PfCLK-KO vectors were observed. DNA was isolated from blasticidin-resistant Myc-tag vector populations, and PCR revealed that integration of the vectors had occurred within 60–90 days post-transfection (Fig. 4, right panels). This was confirmed by Southern blot analysis for *PfCLK-1/Lammer* (Fig. 5A,B) and *PfCLK-2*

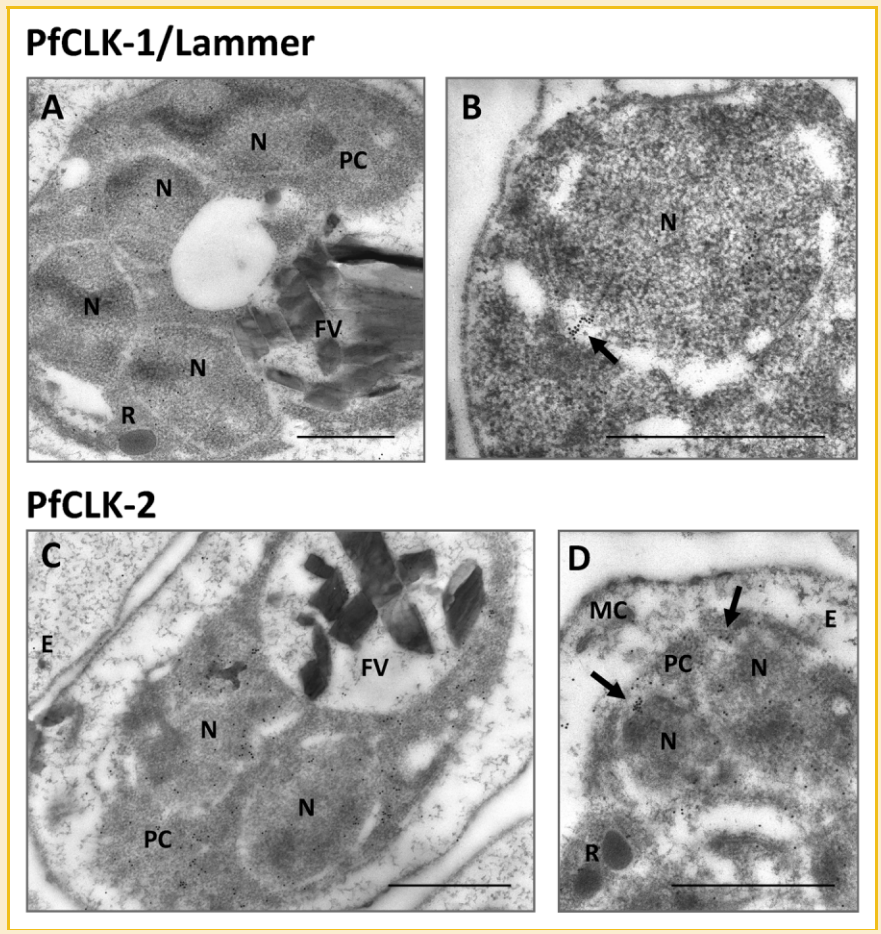

Fig. 3. Ultrastructural localization of PfCLKs in the parasite blood stages. Post-embedding immunoelectron microscopy labeling was performed using mouse antisera against PfCLK-1/Lammer and PfCLK-2, respectively, in combination with secondary gold-conjugated antibody. A: PfCLK-1/Lammer is predominantly present in the nucleus of a blood stage schizont. B: A distinct labeling of PfCLK-1/Lammer in the passage between nucleus and cytoplasm (arrow) was detected in another schizont. C: PfCLK-2 is expressed in the nucleus as well as the cytoplasm of a late trophozoite. D: PfCLK-2 labeling was particularly detected in the passage between nucleus and cytoplasm (arrows) of a schizont. E, erythrocyte; FV, food vacuole; MC, Maurer's cleft; N, nucleus; PC, parasite cytoplasm; R, rhoptry. Bar: 0.5 μm.

TABLE I. Quantification of Gold-Labeling of PfCLKs in Ultrasections of Blood Stage Parasites

		Blood stage parasite					Erythrocyte
		R	FV	N	Cyt	Total	Total
PfCLK-1/Lammer							
# 1	T	N/A	0	15	20	35	25
# 2	ES	1	N/A	16	26	43	13
# 3	ES	2	1	27	34	64	18
# 4	ES	0	N/A	20	32	52	28
# 5	T	N/A	N/A	8	15	23	10
# 6	ES	1	3	38	29	71	16
# 7	ES	0	7	35	65	107	38
# 8	ES	0	1	32	47	80	44
# 9	T	N/A	1	28	32	61	10
# 10	ES	0	N/A	36	22	58	12
PfCLK-2							
# 1	T	N/A	0	38	36	74	17
# 2	ES	3	N/A	75	58	136	28
# 3	T	N/A	6	38	74	118	37
# 4	T	N/A	1	81	50	132	23
# 5	T	N/A	9	44	102	155	33
# 6	T	N/A	0	17	31	48	7
# 7	T	N/A	N/A	15	27	42	9
# 8	T	N/A	N/A	89	30	119	10
# 9	T	N/A	10	31	48	89	17
# 10	ES	0	N/A	41	31	72	11

Cyt, cytoplasm; ES, early schizont; FV, food vacuole; N, nucleus; N/A, not applicable; R, rhoptry; T, trophozoite.

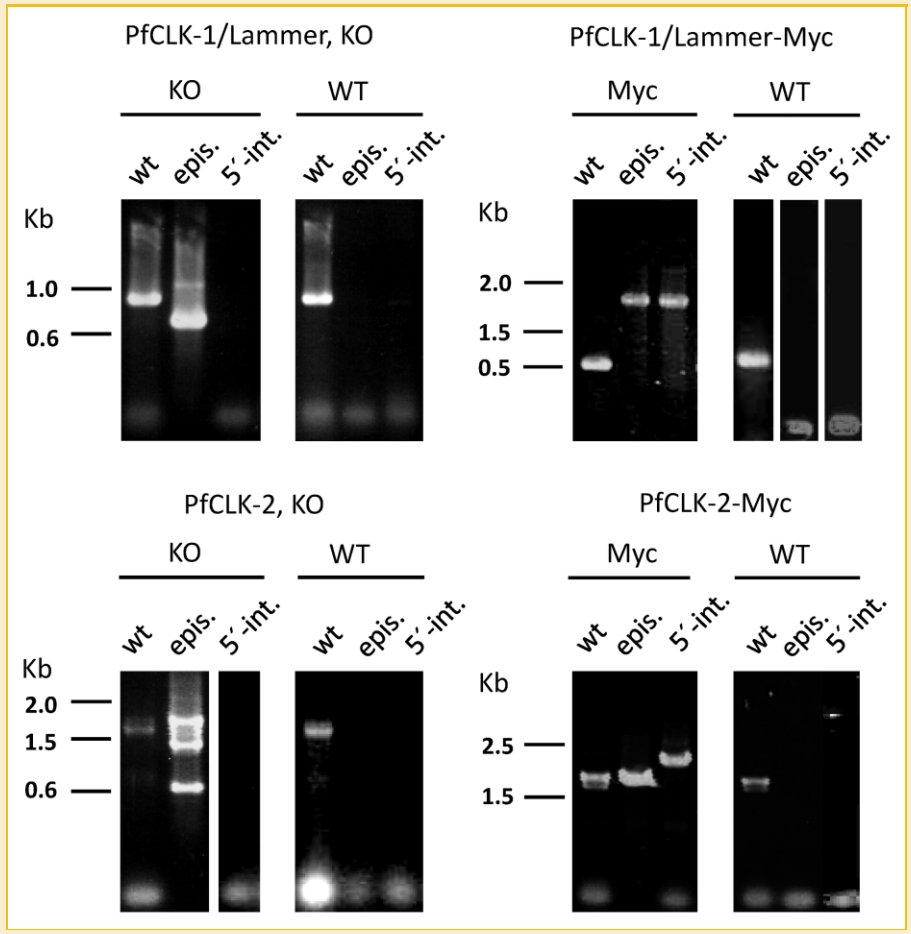

Fig. 4. Molecular analysis of reverse genetics mutations in *PfCLK* genes. Diagnostic PCR from the gDNA isolated from parasites transfected with the PfCLK-1-KO-vector showed amplification bands correlating to the wild-type (WT) gene locus (977 bp) and episome (672 bp), but no band for 5′-integration of the vector at 20 weeks post-transfection. Untransfected wild-type 3D7 parasites were used as a positive control for the WT gene locus and as a negative control for 5′-integration. Similarly, only bands for the WT gene locus (1.631 kb) and episome (652 bp), but no band for 5′-integration were detected, when gDNA from parasites transfected with the PfCLK-2-KO-vector was investigated. Recombinogenicity of the *PfCLK-1/Lammer* gene locus by integration of the PfCLK-1-Myc vector at 60 days post-transfection was shown by diagnostic PCR, revealing bands for episome (1.93 kb) and 5′-integration (1.92 kb) together with bands for the *PfCLK-1/Lammer* WT gene locus (534 bp) from gDNA of transfected mixed cultures. Similarly, recombination of the PfCLK-2-Myc vector was identified by bands for episome (1.67 kb) and 5′-integration (2.34 kb) together with bands for the *PfCLK-2* WT gene locus (1.63 kb). For control, gDNA from untransfected WT parasites was used.

(Fig. 6A,B). The WT locus had disappeared from the (uncloned) blasticidin-resistant population, as was previously described for Pfmap-2 [Dorin-Semblat et al., 2007].

The presence of Myc-tagged proteins in the transgenic populations was demonstrated by Western blot analysis on lysates of Myc-tagged mixed cultures. For PfCLK-1/Lammer-Myc, the above-described immunoreactive band of 60 kDa was detectable using antibodies against the Myc-tag (Fig. 5C). No protein bands were detected when the anti-Myc antibody was used on lysates of WT 3D7 cultures. Similar 60 kDa protein bands were detected, when lysates of Myc-tagged mixed cultures or WT cultures were probed with anti-PfCLK-1/Lammer antisera in Western blots. Detection of Myc-tagged PfCLK-2 by Western blotting revealed a protein band of 55 kDa, which represents the above-mentioned processing or degradation product corresponding to the C-terminus of PfCLK-2 (Fig. 6C), but no 150 kDa full-length protein band was detectable. When PfCLK-2-Myc parasite lysates or WT lysates were probed with the anti-PfCLK-2 antisera in Western blots, the full-length protein and the above-described lower molecular weight proteins of 70 and 55 kDa were detected. Therefore, the anti-Myc antibody appears to only detect the 55 kDa processed protein of PfCLK-2-Myc.

We subsequently investigated the immunolocalization of PfCLK-Myc mutants in blood stage parasites. Immunofluorescence assay on methanol-fixed mutants, using anti-Myc antibody, showed punctate expression of PfCLK-1/Lammer-Myc in the nuclei of trophozoites and schizonts, while PfCLK-2-Myc was present in the nuclei and the cytoplasm of blood stages (Supplemental Fig. 4A). No labeling was detected in WT blood stages, when these were immunolabeled with the anti-Myc antibody for negative control (data not shown).

Immunoelectron microscopy, using post-embedding labeling, detected PfCLK-1/Lammer-Myc predominantly in the nuclei and PfCLK-2-Myc in the nucleus and cytoplasm of blood stage parasites, when expression of Myc-tagged protein was visualized by gold-

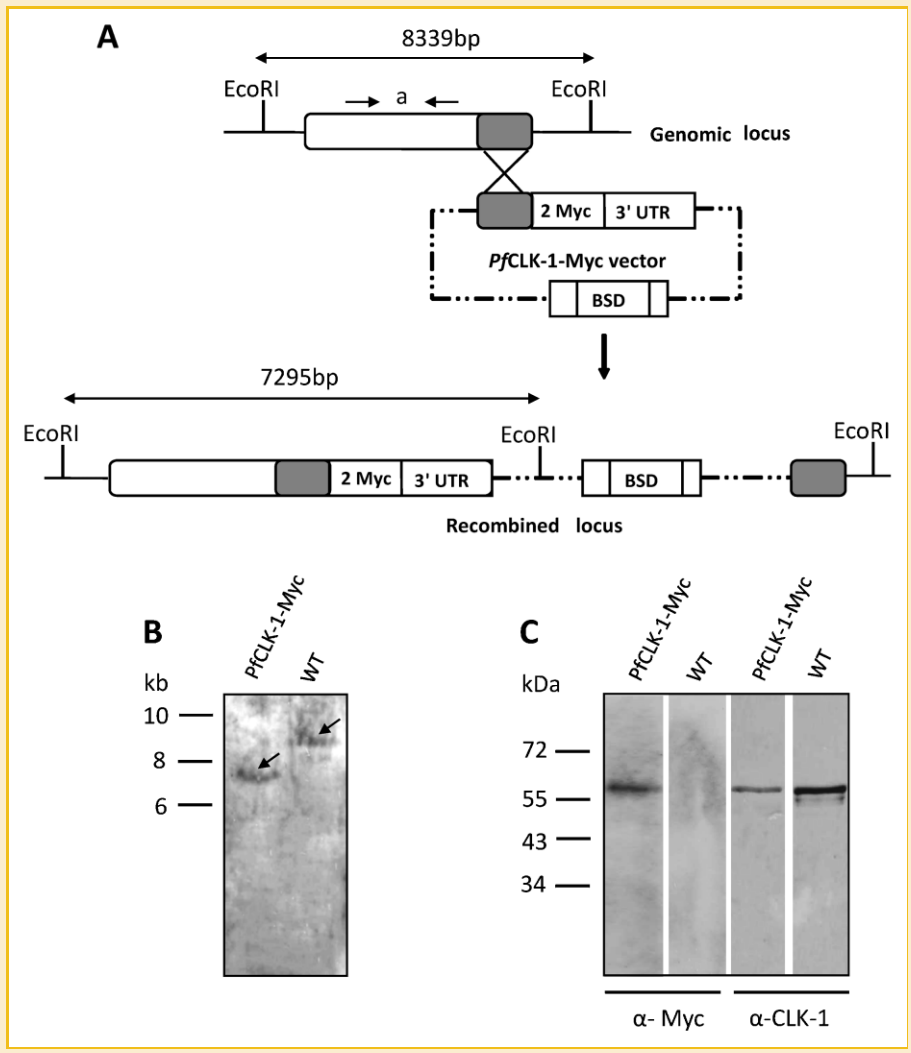

Fig. 5. Molecular analysis of successful PfCLK-1-Myc vector integration. A: Schematic showing integration of the PfCLK-1-Myc vector, location of *Eco*RI restriction sites and of the oligonucleotide probe (a), and size of expected DNA fragments after digestion of wild-type (WT) and mutant gDNA. B: Southern blotting of digested DNA fragments revealed a DNA band indicative of PfCLK-1-Myc vector integration (7,295 bp) for PfCLK-1-Myc parasites. No WT bands were detected. As control, gDNA of non-integrated 3D7 cultures were used and a band indicative for the WT gene locus was detected (8,339 bp). Arrows indicate location of DNA bands. C: Western blot analysis using anti-Myc antibody showed expression of a 60 kDa protein in PfCLK-1-Myc lysate, but no protein band in lysate of non-integrated 3D7 parasites. Probing with anti-PfCLK-1/Lammer antibody resulted in a 60 kDa protein band in both lysates.

labeled secondary antibody (Supplemental Fig. 4B). No gold labeling was found in uninfected erythrocytes or when ultrasections of WT parasites were probed with anti-Myc antibody (data not shown). In summary, the immunolocalization data on the PfCLK-Myc mutants confirm the kinase expression pattern observed in WT parasites (see above).

PfCLK-1/LAMMER AND PfCLK-2 ARE ASSOCIATED WITH PHOSPHORYLATION ACTIVITY

To investigate the phosphorylation activity of PfCLK-1/Lammer and PfCLK-2, the kinases were co-immunoprecipitated from parasite lysates, using the respective mouse antisera. The immunoprecipitated proteins were used in kinase activity assays as described previously [Reininger et al., 2009], adding as substrate histone H1, MBP, or α/β casein, as well as radiolabeled [γ-32P] ATP. Substrate phosphorylation was detected by autoradiography after gel electrophoresis of the reactions. Both precipitated PfCLK-1/Lammer and PfCLK-2 were associated with phosphorylation activity of all three substrates (Fig. 7A, upper panel). Autophosphorylation was not observed for any of the two kinases. Recombinant PfPK6 was used as a positive control [Bracchi-Ricard et al., 2000] and exhibited strong activity. As negative control, the assay was performed without precipitated kinases (Fig. 7A, upper panel). Coomassie blue staining of radio-labeled gels were used for loading control (Fig. 7A, lower panel).

Similar results were obtained, when lysates from mutants expressing Myc-tagged PfCLK-1/Lammer and PfCLK-2 were subjected to immunoprecipitation assays via anti-Myc antibody and used in the kinase activity assays (Supplemental Fig. 5, upper panel). Both immunoprecipitates phosphorylated histone H1, MBP, and α/β casein, while much weaker signals were obtained with

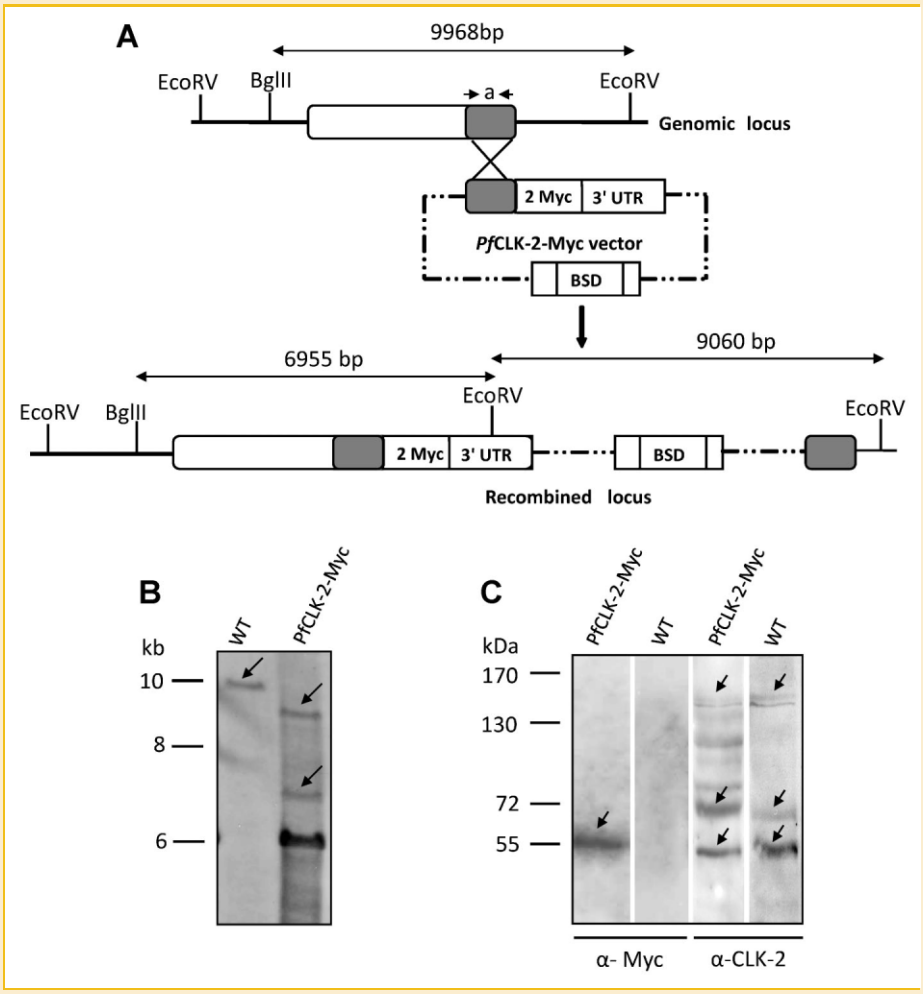

Fig. 6. Molecular analysis of successful PfCLK-2-Myc vector integration. A: Schematic showing integration of the PfCLK-2-Myc vector, location of *Eco*RV and *Bgl*II restriction sites and of the oligonucleotide probe (a), and size of expected DNA fragments after digestion of wild-type (WT) and mutant gDNA. B: Southern blotting of digested DNA fragments revealed two DNA bands indicative of PfCLK-2-Myc vector integration (9,060 and 6,955 bp) for PfCLK-2-Myc mutant parasites. An episomal DNA band at approximately 6,000 bp was additionally detected. No WT bands were detected. As control, gDNA of non-integrated 3D7 cultures were used and a band indicative for the WT gene locus was detected (9,968 bp). Arrows indicate location of DNA bands. C: Western blot analysis, using anti-Myc antibody, showed expression of a 55 kDa protein in PfCLK-2-Myc lysate (arrow), but no protein band in lysate of non-integrated 3D7 parasites. Probing with anti-PfCLK-2 antibody resulted in a 150 kDa full size protein band, as well as in smaller protein bands, particularly running at 70 kDa and 55 kDa (arrows).

immunoprecipitates obtained from extracts of WT 3D7 parasites (Supplemental Fig. 5, upper panel). Coomassie blue staining of radiolabeled gels were used for loading control (Supplemental Fig. 5, lower panel).

As described above, the two kinases exhibit similarities in the substrate-binding site with yeast Sky1p, which has a specific substrate, the SR-rich splicing factor Npl3p. We therefore used recombinant GST-tagged Npl3p as a substrate in the in vitro kinase activity assays. Immunoprecipitated PfCLK-1/Lammer and PfCLK-2 phosphorylated Npl3p (Fig. 7B), which was running at a molecular weight of approximately 95 kDa in the SDS gel. An additional phosphorylation signal of approximately 60 kDa represents truncated GST-tagged Npl3p recombinant protein, as verified by Western blotting using anti-GST antibody (data not shown). A more intense phosphorylation signal was observed when Npl3p was preincubated with the parasite lysate prior to precipitation by anti-PfCLK-1/Lammer antibody, indicating that the kinase forms a stable complex with the splicing factor (Fig. 7B).

We searched for possible *P. falciparum* PfCLK substrates by comparing amino acid sequences in silico and identified a number of putative splicing factors with homology to yeast Npl3p and to the human CLK kinase substrate, ASF/SF2 [Lamond, 1991]. These included the putative plasmodial ortholog of the alternative splicing factor ASF-1 (PF11_0205), which showed 42% identity with the amino acid sequences of ASF/SF2. Recombinant GST-tagged PfASF-1 (48 kDa) was used as substrate in the kinase activity assays and was phosphorylated by both PfCLK kinases (Fig. 7B, upper panel). The combined data indicate that the PfCLKs are able to phosphorylate SR-rich splicing factors in vitro. No signal was observed when GST alone was added to the assay (Fig. 7B, upper panel). Coomassie blue staining of radiolabeled gels were used for loading control (Fig. 7B, lower panel).

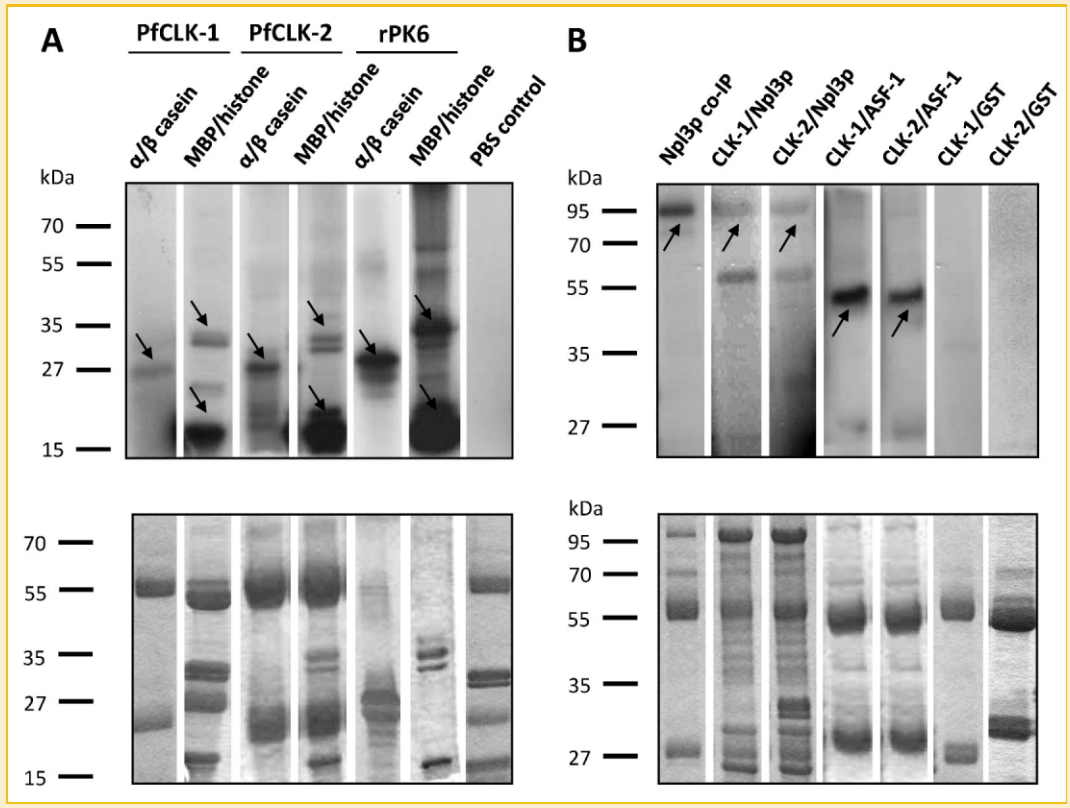

Fig. 7. Kinase activity assay on immunoprecipitated PfCLKs. A: PfCLKs were immunoprecipitated and used in kinase activity assays together with radiolabeled [γ-32P] ATP. The autoradiography (upper panel) of SDS gel separated proteins revealed phosphorylation of the substrates histone H1, MBP, and casein (~33, 18, and 28 kDa; indicated by arrows) by immunoprecipitated PfCLK-1/Lammer or PfCLK-2. Assays without precipitated proteins (PBS control) were used for negative controls. Recombinant rPK6 as positive control resulted in intense substrate phosphorylation. Coomassie blue staining (lower panel) of radiolabeled gels was used as a loading control. B: Kinase activity assays on immunoprecipitated PfCLKs resulted in phosphorylation of GST-tagged Npl3p and PfASF-1 by both kinases (running at approximately 95 and 48 kDa, respectively; indicated by arrows; upper panel). An additional phosphorylation signal of truncated GST-tagged Npl3p was visible at approximately 60 kDa. An intense phosphorylation signal of 95 kDa was observed, when Npl3p was preincubated with parasite lysate prior to co-immunoprecipitation with anti-PfCLK1/Lammer antibody. GST-tag alone (26 kDa) as substrate was used as negative control. Coomassie blue staining (lower panel) of radiolabeled gels was used as a loading control.

PfCLK-1/LAMMER AND PfCLK-2 ASSEMBLE WITH PROTEINS INDICATIVE OF NUCLEID ACID PROCESSING AND SIGNALING

In other organisms, CLKs act in a protein complex, when phosphorylating SR-rich splicing factors, which assemble around and accompany mRNA during processing. In a final set of experiments, we therefore aimed at identifying potential interaction partners of the two PfCLKs in order to identify potential components of these complexes. Co-immunoprecipitation assays on lysates of asexual 3D7 parasite cultures using mouse polyclonal antibodies against PfCLK-1/Lammer or PfCLK-2 were performed to isolate the respective kinases as well as proteins that have bound to these enzymes. Precipitated proteins were then separated by SDS–PAGE and visualized via colloidal Coomassie. Co-immunoprecipitation assays on lysates of uninfected erythrocytes using the same antibodies were used as negative controls, and band patterns were compared between samples of parasite and erythrocyte lysates. Selected protein bands were then subjected to mass spectrometric analysis, and detected peptides were subsequently used for MASCOT searches to identify full-length proteins (settings in experimental procedures). Proteins detected with a high degree of confidence were then annotated via PlasmoDB, SMART, and NCBI Blast programmes. Because genes are often arranged in functional clusters, we further investigated genes adjacent to the gene of interest.

Co-immunoprecipitation of PfCLK-1/Lammer followed by mass spectrometry identified one putative interaction partner, the gene product of PF14_0117 (Table II). This gene encodes for a 39 kDa protein comprising a signal peptide and a conserved phospholipase C/P1 nuclease domain. Its paralog PF14_0119 encodes for a putative p1/s1 nuclease and the *P. yoelii* ortholog PY00427 for a 3′nucleotidase/nuclease.

When PfCLK-2 was used as bait for co-immunoprecipitation, five potential interaction partners were identified (Table II). The protein with the highest molecular weight, which assembled with PfCLK-2, is the gene product of PFL1445w. The gene encodes for a 241 kDa protein with a predicted transmembrane segment and a conserved domain similar to cell cycle control phosphatase. Genome annotation further indicated a TBC domain (Tre-2, Bub2, and Cdc16 domain) with GTPase-activation activity. We also identified the gene product of PF13_0187, which encodes for a conserved protein of 159 kDa showing domain similarities with viral RNA helicase. Its ortholog PY01409 in *P. yoelii* is an assigned ATP-dependent DNA replication helicase DNA2.

TABLE II. Mass Spectrometric Identification of PfCLK-Binding Putative Proteins

Gene ID	Co-IP with	MW (kDa)	Annotated domains	Paralog	Ortholog	Gene cluster
PF14_0117	PfCLK-1/ Lammer	39	Phospholipase C/P1 nuclease	PF14_0119 p1/s1 nuclease	PY00427 (3′ nucleotidase/ nuclease)	PF14_0114 (GTP-binding protein); PF14_0122 (nuclear transport factor)
PFL1445w	PfCLK-2	241	TMD; TBC; cell cycle control phosphatase	N/A	N/A	PFL1465c (heat shock protein)
PF13_0187	PfCLK-2	159	Nucleoside triphosphate hydrolase; RNA helicase	N/A	PY01409 (DNA replication helicase DNA2)	PF13_0185 (histone H3)
PFI1190w	PfCLK-2	128	N/A	N/A	N/A	PFI1175c (RNA-binding protein; PFI1180c (patatin-like phospholipase; PFI1195c (thiamine pyrophospholipase)
PF11_0084	PfCLK-2	84	N/A	N/A	N/A	PF11_0083 (RNA-binding protein)
PFL1220w	PfCLK-2	41	N/A	N/A	N/A	N/A
PF14_0598	PfCLK-1/Lammer; PfCLK-2	37	GAPDH	N/A	N/A	N/A

IP, immunoprecipitation; N/A, not applicable; MW, molecular weight; PF, *Plasmodium falciparum*; PY, *Plasmodium yoelii*; RNA, ribonucleic acid; TBC, Tre-2, Bub2, and Cdc16 domain; TMD, transmembrane domain.

Three more proteins were identified, for which no conserved domains could be annotated. Firstly, the gene product of PFI1190w encodes for a protein (128 kDa) without any assigned function. The gene, however, lies on chromosome 9 within a cluster of genes, encoding for a RNA-binding protein (PFI1175c), a patatin-like phospholipase (PFI1180c), and a thiamine pyrophospholipase (PFI1195c). Further PF11_0084 encodes for a 84 kDa protein of unknown function. Noteworthy, the gene lies on chromosome 11 next to the gene for a putative nucleic acid-binding protein, PF11_0083. Lastly, the gene PFL1220w encodes for a protein (41 kDa) of unknown function.

Mass spectrometry also led to the identification of glyceraldehyde-3-phosphate dehydrogenase (PF14_0598; 37 kDa) in both samples (Table II). The presence of this abundantly expressed metabolic enzyme might be due to unspecific binding during co-immunoprecipitation.

DISCUSSION

Previous analysis of the *P. falciparum* genome sequence identified 65 parasite-encoded kinases, the majority of which belonged to the CMGC group [Ward et al., 2004; Anamika et al., 2005], among them six members of the CDK family. Interestingly, four additional enzymes, PF14_0431, PF14_0408, PF11_0156, and PFC0105w, cluster with the human kinases involved in mRNA-splicing processes, like the SR-rich pre-mRNA splicing factor phosphorylating human kinases SRPK1 through SRPK3 or the human LAMMER kinases CLK1-4 [Ward et al., 2004]. These kinases are reported to phosphorylate SR-rich splicing factors involved in mRNA processing, thereby causing their redistribution and release into the nucleoplasm [Colwill et al., 1996]. The four parasite enzymes were thus termed *P. falciparum* CLK, PfCLK-1-4. Of the four proteins, PF14_0431 was the first one to be identified as a homolog of human Lammer kinase hCLK-1 [Li et al., 2001], while PfCLK-4 was recently functionally characterized as splicing-related PfSRPK1 [Dixit et al., 2010].

In this study, we focused on two of the above-mentioned CLK kinases, which both possess nuclear localization signal sites, and which are here termed PfCLK-1/Lammer and PfCLK-2. Both enzymes align with the *Saccharomyces cerevisae* kinase Sky1p that has been reported to be involved in mRNA splicing and shuttle [Siebel et al., 1999]. The two PfCLKs are predicted to be localized in the parasite nuclear speckles, dynamic structures within the nucleus, where pre-mRNA splicing factors are localized and then recruited to sites of transcription [reviewed in Spector, 2001].

Transcript expression analysis indicated PfCLK expression in the parasite blood stages. Confocal laser scanning and immunoelectron microscopy revealed that the two kinases are located in the nucleus of blood stage parasites. Particularly PfCLK-1/Lammer was detectable in nuclear substructures, consistent with the notion that the kinase is located in the nuclear speckles. On the ultrastructural level, both kinases were repeatedly detected in passages between nucleus and cytoplasm, suggesting that they function in mRNA transport, as was reported for the yeast mRNA splicing kinase Sky1p [Siebel et al., 1999]. Expression of PfCLK-2 was not restricted to the nucleus, but the kinase was also present in the cytoplasm, similar to the expression pattern recently described for SRPK1 [Dixit et al., 2010]. PfCLK-1/Lammer and PfCLK-2 were further found in gametocytes, sexual stage precursor cells that mediate parasite transition to the mosquito.

Endogenous precipitated proteins revealed phosphorylation activity, when exogenous substrates were added in the presence of ATP. The two kinases were further able to phosphorylate the Sky1p substrate Npl3p, a SR-like protein that becomes phosphorylated at a single C-terminal Serine residue [Lukasiewicz et al., 2007], as well as the plasmodial homolog of the splicing factor ASF-1. Interestingly, an intense phosphorylation signal was observed, when Npl3p was preincubated with the parasite lysate prior to precipitation of endogenous PfCLK-1/Lammer, indicating the kinase forms a stable complex with the splicing factor. Other components, including additional kinases, might participate in this complex, which would explain the increased intensity of the phosphorylation signal.

The combined expression and activity data led us to hypothesize that the two kinases play important roles for the parasite blood stages, and we therefore performed functional analysis studies to determine kinase essentiality. The functional characterization of kinases with essential roles in the blood stage replication cycle represents a major challenge due to the fact that these kinases

cannot be knocked out and that no phenotype characterization can therefore be performed. In these cases, reverse genetics approaches can indirectly prove the essentiality of the gene. The inability to KO a kinase gene locus, together with the ability to modify the allele in a way that does not cause loss-of-function of the gene product, are strongly indicative of an important role during asexual blood stages. This approach initially led to the identification of Pbcrk-1, a CDK-related kinase, as likely to be essential for schizogony in *P. berghei* [Rangarajan et al., 2006]. Reverse genetics approaches were subsequently applied to reveal an essential blood stage function for the *P. falciparum* kinases Pfmap-2 [Dorin-Semblat et al., 2007], PfCK2 [Holland et al., 2009], Pfcrk-3 [Halbert et al., 2010], and PfTKL3 [Abdi et al., 2010].

Using a similar reverse genetics approach we here show that PfCLK-1/Lammer and PfCLK-2 possess important roles for erythrocytic schizogony. We were not able to KO either of the two gene loci by homologous single-crossover recombination, while isochronously the locus of the *P. falciparum* kinase, PFC0485w (homolog of *P. berghei* PKRP [Purcell et al., 2010]) was disrupted by the same strategy. Insertions of sequences at the 3′end of the kinases, on the other hand, which allow tagging of the gene product without affecting enzymatic activity, were feasible and resulted in the expression of Myc-tagged proteins.

In conclusion we showed that PfCLK-1/Lammer and PfCLK-2 (1) exhibit homology with a eukaryotic kinase involved in phosphorylation of SR proteins during pre-mRNA processing; (2) are present in the parasite nucleus and in the passage between nucleus and cytoplasm; (3) exhibit in vitro phosphorylation activity, including phosphorylation of the yeast SR-rich splicing factor Npl3p and of the plasmodial substrate PfASF-1, a putative splicing factor; and (4) are crucial for completion of the erythrocytic asexual cycle. In accord with these data we propose that PfCLK-1/Lammer and PfCLK-2 function in the phosphorylation of plasmodial SR-rich splicing factors during mRNA splicing and shuttle.

From their initial transcription in the nucleus until translation at the rough endoplasmic reticulum, mRNA molecules are dynamically associated with proteins of messenger ribonucleoprotein particles (mRNPs), which mediate capping, splicing, and polyadenylation. Many mRNP proteins are subject to phosphorylation, which regulates binding and activity of these factors [reviewed in Huang and Steitz, 2005]. Of particular importance are the SR proteins that function in pre-mRNA splicing. SR proteins, when not in action, reside in the nuclear speckle, but shuttle between the nucleus and the cytoplasm during splicing. The activity of SR proteins is controlled by an interplay of phosphorylating CLK kinases and dephosphorylating phosphatases, and only dephosphorylated splicing factor appears to accompany mRNA from the nucleus to the cytoplasm, while rephosphorylation facilitates its release from the mRNPs [Gilbert and Guthrie, 2004].

The control of transcript modification is an important process in *P. falciparum* due to the role of post-transcriptional regulation of expression of the intron-rich parasite genes. However, up to date, the modes of action of mRNA splicing and the composition of mRNPs remain largely unknown. A new study uncovered the composition of a gametocyte-specific mRNP in *P. berghei*, which functions in storing translationally silent mRNA critical for post-fertilization development of the malaria parasite [Mair et al., 2010]. In an attempt to identify potential components of the complexes involved in mRNA splicing and transport in the *P. falciparum* blood stages, we performed mass spectrometric analysis on binding partners for the two PfCLKs. Since hitherto most malaria mRNP components are unknown, all of the identified proteins were considered hypothetical. Annotation of some of these proteins predicted roles in nucleic acid processing and signal transduction. These include proteins with putative nuclease, phosphatase, or helicase functions. Our findings form the basis for future studies on unveiling the malaria spliceosome, which might represent a chemotherapeutic target due to its essentiality for the malaria parasite.

ACKNOWLEDGMENTS

This study was supported by EU 7th Framework Programme Grants MALSIG (to G.P. and C.D.); ANTIMAL (to C.D.); and EVIMALAR (to C.D.), Deutsche Forschungsgemeinschaft PR905/1 (Emmy Noether Programme, to G.P.); SFB544/B2; SFB630/C6 (to T.D.) and SFB593/B7/Z2 (to Klaus Lingelbach, University of Marburg), and Inserm, EPFL (to C.D.). We are grateful to Gourisankar Ghosh (University of California, San Diego) for providing GST-tagged Npl3p, to David Fidock (Columbia University, New York) for providing the pCAM-BSD plasmid, and to Pietro Alano (Istituto Superiore di Sanità, Rome) for providing strain F12. We thank Armin Robubi (University of Würzburg) for support with the bioinformatic analysis and Nadja Braun (University of Marburg) and Ludmilla Sologub (University of Würzburg) for excellent technical assistance. S.A. was supported by the BioMedTec International Graduate School of Science ''Lead structures of cell function'' of the Elite Network Bavaria.

REFERENCES

Abdi A, Eschenlauer S, Reininger L, Doerig C. 2010. SAM domain-dependent activity of PfTKL3, an essential tyrosine kinase-like kinase of the human malaria parasite *Plasmodium falciparum*. Cell Mol Life Sci 67(19):3355–3369.

Anamika, Srinivasan N, Krupa A. 2005. A genomic perspective of protein kinases in *Plasmodium falciparum*. Proteins 58(1):180–189.

Bracchi-Ricard V, Barik S, Delvecchio C, Doerig C, Chakrabarti R, Chakrabarti D. 2000. PfPK6, a novel cyclin-dependent kinase/mitogen-activated protein kinase-related protein kinase from *Plasmodium falciparum*. Biochem J 347(1):255–263.

Cohen P. 2001. The role of protein phosphorylation in human health and disease. The Sir Hans Krebs Medal Lecture. Eur J Biochem 268(19):5001–5010.

Colwill K, Pawson T, Andrews B, Prasad J, Manley JL, Bell JC, Duncan PI. 1996. The Clk/Sty protein kinase phosphorylates SR splicing factors and regulates their intranuclear distribution. EMBO J 15(2):265–275.

Deitsch K, Duraisingh M, Dzikowski R, Gunasekera A, Khan S, Le Roch K, Llinas M, Mair G, McGovern V, Roos D, Shock J, Sims J, Wiegand R, Winzeler E. 2007. Mechanisms of gene regulation in *Plasmodium*. Am J Trop Hyg 77(2):201–208.

Dixit A, Singh PK, Sharma GP, Malhotra P, Sharma P. 2010. PfSRPK1, a novel splicing-related kinase from *Plasmodium falciparum*. J Biol Chem 285(49):38315–38323.

Doerig C. 2004. Protein kinases as targets for anti-parasitic chemotherapy. Biochim Biophys Acta 1697(1–2):155–168.

Doerig C, Meijer L. 2007. Antimalarial drug discovery: Targeting protein kinases. Expert Opin Ther Targets 11(3):279–290.

Doerig C, Billker O, Pratt D, Endicott J. 2005. Protein kinases as targets for antimalarial intervention: Kinomics, structure-based design, transmission-blockade, and targeting host cell enzymes. Biochim Biophys Acta 1754(1–2): 132–150.

Dorin-Semblat D, Quashie N, Halbert J, Sicard A, Doerig C, Peat E, Ranford-Cartwright L, Doerig C. 2007. Functional characterization of both MAP kinases of the human malaria parasite *Plasmodium falciparum* by reverse genetics. Mol Microbiol 65(5):1170–1180.

Dorin-Semblat D, Sicard A, Doerig C, Ranford-Cartwright L, Doerig C. 2008. Disruption of the PfPK7 gene impairs schizogony and sporogony in the human malaria parasite *Plasmodium falciparum*. Eukaryot Cell 7(2):279–285.

Francis SE, Gluzman IY, Oksman A, Knickerbocker A, Mueller R, Bryant ML, Sherman DR, Russell DG, Goldberg DE. 1994. Molecular characterization and inhibition of a *Plasmodium falciparum* aspartic hemoglobinase. EMBO J 13(2):306–317.

Fraunholz MJ, Roos DS. 2003. PlasmoDB: Exploring genomics and post-genomics data of the malaria parasite, *Plasmodium falciparum*. Redox Rep 8(5):317–320.

Gilbert W, Guthrie C. 2004. The Glc7p nuclear phosphatase promotes mRNA export by facilitating association of Mex67p with mRNA. Mol Cell 13(2):201–212.

Godin KS, Varani G. 2007. How arginine-rich domains coordinate mRNA maturation events. RNA Biol 4(2):69–75.

Halbert J, Ayong L, Equinet L, Roch KL, Hardy M, Goldring D, Reininger L, Waters N, Chakrabarti D, Doerig C. 2010. A *Plasmodium falciparum* transcriptional CDK-related kinase with a crucial role in parasite proliferation associates with histone deacetylase activity. Eukaryot Cell 9(6):952–959.

Hanks SK, Quinn AM. 1991. Protein kinase catalytic domain sequence database: Identification of conserved features of primary structure and classification of family members. Methods Enzymol 200:38–62.

Hellmann U, Wernstedt C, Gonez J, Heldin CH. 1995. Improvement of an "In-Gel" digestion procedure for the micropreparation of internal protein fragments for amino acid sequencing. Anal Biochem 224(1):451–455.

Higgins DG, Thompson JD, Gibson TJ. 1996. Using CLUSTAL for multiple sequence alignments. Methods Enzymol 266:383–402.

Holland Z, Prudent R, Reiser JB, Cochet C, Doerig C. 2009. Functional analysis of protein kinase CK2 of the human malaria parasite *Plasmodium falciparum*. Eukaryot Cell 8(3):388–397.

Huang Y, Steitz JA. 2005. SRprises along a messenger's journey. Mol Cell 17(5):613–615.

Hyde JE. 2005. Drug-resistant malaria. Trends Parasitol 21(11):494–498.

Ifediba T, Vanderberg JP. 1981. Complete *in vitro* maturation of *P. falciparum* gametocytes. Nature 294(5839):364–366.

Kaslow DC, Quakyi IA, Syin C, Raum MG, Keister DB, Coligan JE, McCutchan TF, Miller LH. 1988. A vaccine candidate from the sexual stage of human malaria that contains EGF-like domains. Nature 333(6168):74–76.

Lamond AI. 1991. ASF/SF2: A splice site selector. Trends Biochem Sci 16(12):452–453.

Letunic I, Copley RR, Pils B, Pinkert S, Schultz J, Bork P. 2006. SMART 5: Domains in the context of genomes and networks. Nucleic Acids Res 34(Database issue):D257–D260.

Li JL, Targett GAT, Baker DA. 2001. Primary structure and sexual stage-specific expression of a LAMMER protein kinase of *Plasmodium falciparum*. Int J Parasitol 31(4):387–392.

Lukasiewicz R, Nolen B, Adams JA, Ghosh G. 2007. The RGG domain of Npl3p recruits Sky1p through docking interactions. J Mol Biol 367(1):249–261.

Mair GR, Lasonder E, Garver LS, Franke-Fayard BM, Carret CK, Wiegant JC, Dirks RW, Dimopoulos G, Janse CJ, Waters AP. 2010. Universal features of post-transcriptional gene regulation are critical for *Plasmodium* zygote development. PLoS Pathog 6(2):e1000767.

Nair R, Rost B. 2005. Mimicking cellular sorting improves prediction of subcellular localization. J Mol Biol 348(1):85–100.

Nayler O, Stamm S, Ullrich A. 1997. Characterization and comparison of four serine- and arginine-rich (SR) protein kinases. Biochem J 326(3):693–700.

Nolen B, Yun CY, Wong CF, McCammon JA, Fu XD, Ghosh G. 2001. The structure of Sky1p reveals a novel mechanism for constitutive activity. Nat Struct Biol 8(2):176–183.

Nunes MC, Goldring JP, Doerig C, Scherf A. 2007. A novel protein kinase family in *Plasmodium falciparum* is differentially transcribed and secreted to various cellular compartments of the host cell. Mol Microbiol 63(2):391–403.

Peterson MG, Marshall VM, Smythe JA, Crewther PE, Lew A, Silva A, Anders RF, Kemp DJ. 1989. Integral membrane protein located in the apical complex of *Plasmodium falciparum*. Mol Cell Biol 9(7):3151–3154.

Pradel G, Hayton K, Aravind L, Iyer L, Abrahamsen MS, Bonawitz A, Mejia C, Templeton TJ. 2004. A multi-domain adhesion protein family expressed in *Plasmodium falciparum* gametocytes is essential for sporozoite midgut to salivary gland transition. J Exp Med 199(11):1533–1544.

Purcell LA, Leitao R, Ono T, Yanow SK, Pradel G, Spithill TW, Rodriguez A. 2010. A putative kinase related protein (PKRP) from *Plasmodium berghei* mediates infection in the midgut and salivary glands of the mosquito. Int J Parasitol 40(8):979–988.

Rangarajan R, Bei A, Henry N, Madamet M, Parzy D, Nivez MP, Doerig C, Sultan A. 2006. Pbcrk-1, the *Plasmodium berghei* orthologue of *P. falciparum* cdc-2 related kinase-1 (Pfcrk-1), is essential for completion of the intraerythrocytic asexual cycle. Exp Parasitol 112(3):202–207.

Reininger L, Tewari R, Fennell C, Holland Z, Goldring D, Ranford-Cartwright L, Billker O, Doerig C. 2009. An essential role for the plasmodium Nek-2 Nima-related protein kinase in the sexual development of malaria parasites. J Biol Chem 284(31):20858–20868.

Sanford JR, Ellis J, Cáceres JF. 2005. Multiple roles of arginine/serine-rich splicing factors in RNA processing. Biochem Soc Trans 33(3):443–446.

Sayers EW, Barrett T, Benson DA, Bolton E, Bryant SH, Canese K, Chetvernin V, Church DM, Dicuccio M, Federhen S, Feolo M, Geer LY, Helmberg W, Kapustin Y, Landsman D, Lipman DJ, Lu Z, Madden TL, Madej T, Maglott DR, Marchler-Bauer A, Miller V, Mizrachi I, Ostell J, Panchenko A, Pruitt KD, Schuler GD, Sequeira E, Sherry ST, Shumway M, Sirotkin K, Slotta D, Souvorov A, Starchenko G, Tatusova TA, Wagner L, Wang Y, John Wilbur W, Yaschenko E, Ye J. 2010. Database resources of the National Center for Biotechnology Information. Nucleic Acids Res 38:D5–D16.

Sidhu AB, Valderramos SG, Fidock DA. 2005. pfmdr1 mutations contribute to quinine resistance and enhance mefloquine and artemisinin sensitivity in *Plasmodium falciparum*. Mol Microbiol 57(4):913–926.

Siebel CW, Feng L, Guthrie C, Fu XD. 1999. Conservation in budding yeast of a kinase specific for SR splicing factors. Proc Natl Acad Sci USA 96(10): 5440–5445.

Simon N, Scholz SM, Moreira C, Templeton TJ, Kuehn A, Dude MA, Pradel G. 2009. Sexual stage proteins form multi-protein complexes in the malaria parasite *Plasmodium falciparum*. J Biol Chem 284(21):14537–14546.

Spector DL. 2001. Nuclear domains. J Cell Sci 114(16):2891–2893.

Templeton TJ, Fujioka H, Aikawa M, Parker KC, Kaslow DC. 1997. *Plasmodium falciparum* Pfs40, renamed Pf39, is localized to an intracellular membrane-bound compartment and is not sexual stage-specific. Mol Biochem Parasitol 90(1):359–365.

Ward P, Equinet L, Packer J, Doerig C. 2004. Protein kinases of the human malaria parasite *Plasmodium falciparum*: The kinome of a divergent eukaryote. BMC Genomics 5(1):79.